

See discussions, stats, and author profiles for this publication at: <https://www.researchgate.net/publication/323266773>

Statistical modelling and optimization of alkaline peroxide oxidation pretreatment process on rice husk cellulosic biomass to enhance enzymatic convertibility and fermentation to e...

Article in *Cellulose* · April 2018

DOI: 10.1007/s10570-018-1714-6

17

6 authors, including:



A.O. Ayeni

Covenant University Ota Ogun State, Nigeria

59 PUBLICATIONS 445 CITATIONS

[SEE PROFILE](#)



Patrick Thabang Sekoai

University of the Witwatersrand

26 PUBLICATIONS 344 CITATIONS

[SEE PROFILE](#)

READS

128



M.O. Daramola

University of Pretoria

182 PUBLICATIONS 1,060 CITATIONS

[SEE PROFILE](#)



Opeyemi Adeeyo

Covenant University Ota Ogun State, Nigeria

16 PUBLICATIONS 150 CITATIONS

[SEE PROFILE](#)

Some of the authors of this publication are also working on these related projects:




DEGRADATION OF OIL DURING FRYING AND ITS EFFECT ON BIODIESEL PRODUCTION [View project](#)



Production of engineering materials [View project](#)

Statistical modelling and optimization of alkaline peroxide oxidation pretreatment process on rice husk cellulosic biomass to enhance enzymatic convertibility and fermentation to ethanol

Augustine Omoniye Ayeni  · Michael Olawale Daramola · Patrick T. Sekoai · Opeyemi Adeeyo · Musa Joel Garba · Ayotunde A. Awosusi

Received: 1 December 2017 / Accepted: 14 February 2018 / Published online: 19 February 2018
© Springer Science+Business Media B.V., part of Springer Nature 2018

Abstract The complex and ordered arrangements of the lignocellulosic materials make them recalcitrant for their conversions to ethanol. Pretreatment is a crucial step in overcoming these hindrances. In this study, a 2³-full factorial design of experiments optimization technique was applied on the alkaline peroxide oxidation pretreatments of rice husks biomass. The low–high levels of the influencing variables on pretreatments were; temperature (100–120 °C), time (1–2 h), % (v/v) H₂O₂ concentration (1–3%). Under the prevailing pretreatments, the optimum conditions were predicted and validated to be 109 °C, 2 h, and 1.38% H₂O₂ which yielded 56% (w/w) cellulose content, 55% (w/w) hemicellulose solubilization, and 48% (w/w) lignin removal. At the established optimum pretreatment conditions, and considering variations in biomass and enzymes loadings, maximum reducing sugars production was 205 mg/g dry biomass at different enzymatic

hydrolysis conditions of 3% biomass loading, hydrolysis temperature of 45 °C, hydrolysis time of 24 h, and 35 FPU/g cellulose enzyme loading. The highest cellulose conversion of 33% yielded 24 g/L ethanol at the end of the first day of saccharification and fermentation. Physical, structural, and morphological investigations on raw and treated materials using tools such as stereomicroscopy, scanning electron microscopy, and fourier transform infrared spectroscopy further revealed the effectiveness of chosen method on rice husks biomass.

Keywords Full factorial design · Alkaline peroxide oxidation · Enzymatic convertibility · Scanning electron microscopy · Cellulosic biomass · Ethanol

Introduction

The largest potential for fuel ethanol is lignocellulosic biomass (Kim and Dale 2004; Zhang and Cai 2008). Lignocellulosic biomass is primarily composed of three biopolymers: cellulose, hemicelluloses and lignin (Binder and Raines 2010). The lignocellulose is bonded together by covalent bonding, various intermolecular bridges, and van der Waals' forces forming a complex structure, making it resistant to enzymatic hydrolysis and insoluble in water (O'Sullivan 1997). Cellulose is a major fraction in lignocellulosic biomass. Cellulosic biomass is abundantly

A. O. Ayeni (✉) · O. Adeeyo · M. J. Garba
Department of Chemical Engineering, College of
Engineering, Covenant University, Km. 10 Idiroko Road,
Canaan land, Ota, Nigeria
e-mail: augustine.ayeni@covenantuniversity.edu.ng;
aoayeni@gmail.com

M. O. Daramola · P. T. Sekoai · A. A. Awosusi
Sustainable Energy and Environment Research Unit,
School of Chemical and Metallurgical Engineering,
Faculty of Engineering and the Built Environment,
University of the Witwatersrand (Wits), Private Bag 3,
2050 Johannesburg, South Africa

present globally and it is renewable. Lignocellulosic materials include varied sources as agricultural residues, woods, herbaceous energy crops, municipal solid wastes, wastes from pulp and paper industry (Jeya et al. 2009; Ayeni et al. 2013a). Lignin is a valuable part after its removal from the biomass during pretreatment. It is about a third of the lignocellulosic complex. It has high energy content and can be generated in large quantities as second generation biorefineries representing a significant quantity for the production of wide range of renewable chemicals (Varanasi et al. 2013; Buzala et al. 2015; Awosusi et al. 2017b). There is presently a growing trend of utilizing lignocellulosic biomass for fuels and chemicals production. However, the production of fuels and chemicals from these feed-stocks involves adequate feedstock preparation, pretreatment, enzymatic conversion, and fermentation steps. Pretreatment is necessary in order to render the lignocellulosic complex accessible for subsequent enzymatic conversions (Saha and Cotta 2007). Pretreatment removes hemicellulose and lignin from the complex thereby affecting cellulose crystallinity, and increasing the porosity for enzymatic digestion (Zhang and Cai 2008). Sugars exist in significant amounts as holocellulose (cellulose and hemicellulose contents) (57–61%) in rice husks. Like other lignocellulosic materials, the use of rice husks biomass as feedstock for bioethanol production has been limited because of the chemical structure of rice husks making it recalcitrant to enzymatic hydrolysis unless it is pretreated to a more accessible form (Nikzad et al. 2013). Alkaline peroxide oxidation pretreatment is known to de-crystallize cellulose (Gould 1985). Hydrogen peroxide during pretreatments acts as a strong oxidizing agent. It readily reacts with lignin and related phenolics in the lignocellulosic complex (Agnemo and Gellerstedt 1979; Lachenal et al. 1980). This reaction yields low molecular weight and water-soluble oxidation products (Bailey and Dence 1969). Hydrogen peroxide plays an important role in the disruption of the biomass complex by releasing lignin from the matrix and increasing the degree of hydration in the cellulose polymer (Gould 1985; Kutsuki and Gold 1982; Forney et al. 1982).

In this study, the influence of process parameters such as temperature, time, and hydrogen peroxide concentration on the pretreatment of rice husks was investigated. The optimization of the pretreatment step was performed by using the two-level-three-

factor (2^3) factorial designs of experiments (DOE). MINITAB 15 (PA, USA) statistical software was explored in the design and analysis of the pretreatment results. DOE are commonly employed in industrial research where process variables influence the response of the system (Kaiser et al. 2013; Onoji et al. 2017). Factorial design of experiments has been used previously (Ayeni et al. 2013a; Bartos et al. 2015) as a useful optimization technique.

The study was carried out to show how effective alkaline peroxide oxidation pretreatment method is on rice husks biomass in the pursuit of lignin reduction, hemicellulose solubilization and cellulose enhancement. Biomass quality parameters were investigated by estimating the proximate, ultimate, and the high heating values of the raw biomass (García et al. 2014; Awosusi et al. 2017a). Furthermore, the study assessed the compositional changes of the delignification, digestibility of the pretreated samples by cellulase enzymes (at varying loadings of 35, 40, 45, and 50 FPU/g cellulose) at the optimized pretreated conditions. Relationship between biomass loadings (2, 3, 4, and 5%) on the enzymatic digestibility of pretreated biomass was also evaluated at the optimized and validated conditions. The fermentability of sugars produced to ethanol using *Saccharomyces cerevisiae* was also investigated. In accessing the impacts of pretreatments, enzymatic conversion and fermentation of treated biomass, the physical, structural, morphological changes brought about by these actions were investigated using stereomicroscopy, scanning electron microscopy (SEM), and Fourier transform infrared spectroscopy analytical methods (FTIR).

Materials and methods

Materials

Rice husk was sourced from a rice milling factory (Wasimi, South West, Nigeria; 6°59'N 3°13'E at 91 m elevation) early April, 2015. The milled materials were dried in a convention oven at 105 °C for 3 h to a dry matter content of 87%. Screened biomass samples ranged from 0.004 mm to 2.36 mm particle sizes. Dried biomass fraction having sieve size of 1.18 mm was used for this study. The dried biomass was stored in plastic bottles and kept at room temperature until the materials were ready for use. All chemicals were of

the analytical grade procured from Sigma-Aldrich (Chemie GmbH).

Statistical design for pretreatments

A two-level-three-factor full factorial design was employed to analyse the main and combined effects of variables on the pretreatment responses (cellulose content, hemicellulose solubilisation, and lignin removal) studied, as well as to develop models with the subsequent optimization of the process. As a result, eight duplicated experimental runs were conducted (Table 1) based on the factorial experiments with three individual variable ranges (low–high levels); temperature (100–120 °C), time (1–2 h), H₂O₂ concentration (1–3%).

The experimental runs were randomized in order to eliminate bias and to create homogenous treatments. The three input variables (factors) chosen were designated as *A* (temperature), *B* (time), *C* (% H₂O₂). The model generated as a function of these variables on the predicted responses of cellulose content, hemicellulose solubilization, and lignin removal is a second-order polynomial and is represented as follows:

$$Y = \alpha_0 + \alpha_1 A + \alpha_2 B + \alpha_3 C + \alpha_{1,2} AB + \alpha_{1,3} AC + \alpha_{2,3} BC \quad (1)$$

The predicted responses are designated as *Y* associated with each factor level combinations; α_0 to $\alpha_{2,3}$ are coefficients to be estimated from regression, they represent the linear, quadratic and cross-products of *A*, *B*, *C* on the responses. Statistical software MINITAB 15 (PA, USA) was used for regression

analysis of experimental data, plotting of response surfaces and to optimize the process parameters. The coefficients in the second-order polynomial (Eq. 1) were estimated using the least squares (LS) estimation method based on a multiple regression technique of the experimentally obtained data. The predicted responses were obtained using Eq. 1. It is assumed that random errors are identically distributed with a zero mean and a common unknown variance in this method. The residual is an estimate of the corresponding value γ_i (the difference between the actual value or the experimental value, X_i and the predicted value as given in Eq. 2;

$$\gamma_i = X_{i, \text{exp}} - X_{i, \text{pred}} \quad (2)$$

The objective of the optimization process is to minimize the sum of the squares of the residuals (the sum of squares of the errors, SSE) (Onoji et al. 2017);

$$\text{SSE} = \sum_{i=1}^n \gamma_i^2 = \sum_{i=1}^n (X_{i, \text{exp}} - X_{i, \text{pred}})^2 \quad (3)$$

n is the number of experimental runs.

The experiments were carried out by a single operator in order to eliminate block effect. The fits of the polynomial models generated were evaluated by considering their coefficients of determination (R^2). The statistical and regression coefficients were evaluated using the analysis of variance (ANOVA; the probability value (*P*) and the *F*-test evaluations).

Pretreatment of raw materials

The raw rice husks biomass was subjected to alkaline peroxide oxidation pretreatment method (Saha and

Table 1 Composition of solid fractions of raw and alkaline peroxide pretreated rice husks (%w/w)

Reaction products	Raw biomass	(1)	(2)	(3)	(4)	(5)	(6)	(7)	(8)
		100 °C 1 h 3% H ₂ O ₂	100 °C 2 h 1% H ₂ O ₂	120 °C 2 h 1% H ₂ O ₂	100 °C 2 h 3% H ₂ O ₂	100 °C 1 h 1% H ₂ O ₂	120 °C 2 h 3% H ₂ O ₂	120 °C 1 h 1% H ₂ O ₂	120 °C 1 h 3% H ₂ O ₂
Dry matter	100	38.99	70.49	56.45	69.95	63.03	54.86	62.42	47.07
Hemicellulose	25.86	19.85	15.61	19.47	17.59	19.22	22.65	22.55	20.24
Cellulose	38.43	45.14	56.09	49.32	50.27	50.91	42.11	42.28	45.36
Lignin	21.94	17.8	18.33	19.1	17.25	16.95	13.36	16.11	18.12
Extractives	6.1	7.44	1.6	5.24	5.82	5.91	11.37	11.29	9.39
Ash	7.67	6.47	6.37	6.87	9.07	7	10.5	7.77	6.93

Cotta 2007; Gould 1985; Ayeni et al. 2013b), in order to understand their fractionations into cellulose, hemicellulose, and lignin in the solid fraction. All pretreatments were investigated by placing biomass slurry in stainless steel pressured vessels that were heated in an oven to the reaction temperature. The biomass pretreatment was carried out using the biomass to liquid ratio of 1:20 (25 g dry biomass to 500 mL total liquid mixture), 1% (v/v) hydrogen peroxide solution and catalyst additions (NaOH) (0.2 g catalyst addition/g dry biomass). The catalyst additions at the same time adjusted the pH of the mixtures to 11.5 (Ayeni et al. 2014; Gould 1985). The temperature remained within the set point value for the reaction time. After each pretreatment, the reactions were stopped and the temperature was allowed to drop to room temperature. The slurries obtained from each pretreatments were recovered and separated into solid and liquid fractions by vacuum filtration. The solid fraction was washed with distilled water until the pH of the liquid approached 7 (Fannie et al. 1998). The total wet weight of the treated biomass was recorded after the washing. A small portion of the treated wet solid was dried in a convention oven at 45 °C to determine the weight loss during the pretreatments, thereby estimating the hemicellulose solubilization and the lignin removal as reported by our previous studies (Ayeni and Daramola 2017; Awosusi et al. 2017a; Ayeni et al. 2013b). The remaining solid fraction was stored frozen for enzymatic digestibility studies of treated biomass to fermentable sugar and subsequent conversion to ethanol. All experiments were conducted in duplicate and the results were averaged for accuracy.

Enzymatic digestibility of washed untreated and treated biomass

The pretreated materials at validated optimum conditions were hydrolysed using cellulase enzymes. The quantity of biomass needed for the enzymatic hydrolysis was determined based on the washed biomass moisture content and cellulose content (Dowe and McMillan 2008). The enzymatic hydrolysis was performed in 50 mL culture tubes. Sodium citrate buffer (5 mL, 0.1 M, pH 4.8) was added to varying quantities of wet pretreated and untreated substrate in the tubes. A commercial preparation of *Trichoderma reesei* cellulase enzyme procured from Sigma-Aldrich

(Chemie GmbH) with an activity of 49.50 FPU/mL was added at the required enzyme loadings. Total mixture was brought up to 20 mL with the aid of deionized water. The enzymatic digestibility of pretreated solids was quantified as fermentable sugars at 2, 24, 72, and 96 h hydrolysis period using the DNS assay method (Miller 1959). DNS reagent of 3 mL was added to 0.5 mL reducing sugar (resulting supernatant from slurry) in test tubes. Then the mixture was heated 100 °C for 15 min using water bath to develop the red-brown color. Subsequently, 1 mL of 40% potassium sodium tartrate (Rochelle salt) solution was added to this mixture to stabilize the color. After cooling to room temperature in ice bath, the absorbance was recorded with a spectrophotometer (UV-1800 Shimadzu, Japan) at 550 nm. Calibration curves (using glucose as a standard) were used to determine the reducing sugar concentrations (Chang et al. 1998). Experiments were conducted in duplicate at 45 °C in a shaking incubator. Variations in enzyme loadings of 35, 40, 45, and 50 FPU/g cellulose (biomass loading was fixed at 2%) were evaluated (Dowe and McMillan 2008). In addition, at the validated optimum predicted responses, biomass loadings of 2, 3, 4, and 5% using constant enzyme loading of 35 FPU/g cellulose were evaluated. After the termination of each hydrolysis period, hydrolysis was stopped by boiling samples for 15 min in a water bath. The samples were centrifuge to remove residual solids and the supernatants were analysed for sugars.

Simultaneous saccharification and fermentation of pretreated solids

Simultaneous saccharification and fermentation (SSF) method was used to investigate the conversion of treated solids to ethanol (Dowe and McMillan 2008). Biomass cellulose loadings of 3% of dry solids loading (Dowe and McMillan 2008; Ayeni et al. 2016a) for a total fermentation mixture of 50 g were considered. The enzyme loading was kept at 35 FPU/g cellulose loading. *Saccharomyces cerevisiae* was cultured at the Department of Biological Sciences laboratory in Covenant University, Nigeria. The inoculums were developed on MYPD (Malt Extract, Yeast Extract, Peptone, Dextrose) medium containing the following ingredients (g/L): malt extract, 3.0; yeast extract, 3.0; peptone, 5.0; glucose, 10.0 (medium was adjusted to pH 4.8 ± 0.2 with citrate buffer (0.05 M)). The

medium components were initially sterilized by steam autoclaving at 121 °C for 30 min. Inoculation flasks were incubated at 30 ± 2.0 °C for 24 h under shaking conditions (130 revolution per minute). Cells were grown to an optical density (OD₆₀₀) at 0.6 (Dowe and McMillan 2008). At the end of each fermentation period 5 mL of mixture was removed and centrifugation was performed at 4500 revolutions per minute for 5 min. Ethanol and glucose analysis were carried out on the supernatant at time intervals of 0, 24, 72 and 96 h to determine ethanol yields and glucose depletion during SSF. Ethanol analysis was evaluated with the method as described by Bennet (Bennet 1971). Glucose was estimated during the SSF by using glucose kit based on the glucose oxidase reaction (GOD-PAP) (Sarita et al. 2009). Effectiveness of SSF process was monitored for the 96 h period by evaluating the total cellulose conversion rate as follows (Xing et al. 2016);

$$\begin{aligned} & \text{Total cellulose conversion rate (\%)} \\ &= \frac{\text{ethanol (g/L)} \times (180/46) + \text{glucose (g/L)} \times 100}{\text{cellulose of pretreated sample (g/L)} \times 1.11} \end{aligned} \quad (4)$$

Proximate and ultimate analysis

The quality of the rice husks raw cellulosic biomass as energy resource was evaluated by considering the moisture, volatile matter (VM) including liquids and tar, fixed carbon (FC), and ash contents. The proximate analysis, which gives the weight fraction of their values resident in the biomass sample, was carried out by three sequential steps of drying, devolatilization in nitrogen, and oxidation in oxygen utilizing thermogravimetric analysis as reported by El-Sayed and Mostafa (2015) and Mani et al. (2010). The samples were evenly distributed over the sample pan with the initial mass kept to be 10 ± 0.1 mg, and were then subjected to a temperature program. Volatile matter, fixed carbon and moisture contents were measured according to ASTM D-5142-02a (Asadieraghi et al. 2014) using a Perkin-Elmer STA 6000 simultaneous thermal analyzer (STA) equipped with Pyris series-STA 6000 instrument viewer software. Both nitrogen purge gas and oxygen for oxidation were operated at 400 k Pascal. Dried samples were kept at 25 °C for 4 min in a nitrogen atmosphere. Moisture content was

taken as the difference in mass when the samples were heated at 85 °C/min until 110 °C, with nitrogen flow rate 45 mL/min. The temperature at 110 °C was held for 5 min. From 110 to 900 °C (the devolution step), a heating rate of 80 °C/min was applied. Temperature was maintained at 900 °C for 5 min. Once a constant weight loss was reached, the final temperature was held constant for 7 min in an oxygen atmosphere to allow for the complete combustion of the remaining char.

The high heating value (HHV) (ASTM D2015) was measured by DryCal oxygen bomb calorimeter equipped with DryCal 2010 software. Carbon and sulphur elemental compositions were determined using a LECO SC632 (equipped with LECO SC632 sulphur/carbon determinator software). The carbon-sulphur analyser was operated at the furnace temperature of 1350 °C. Elemental compositions of hydrogen and nitrogen were determined by using Flash 2000 CHNS/O analyser (Thermo Scientific, USA). Oxygen (wt%) was measured by the difference of C, H, N, S, and ash sum from 100%. The HHV (MJ/kg) experimental value was further compared with the calculated values from established correlations as expressed by Eqs. 5–9. Boie, (1957), Eq. 5, Yin (2011), Eqs. 6 and 9, Jenkins and Ebeling (1985), Eq. 7, Demirbas (1997), Eq. 8. The LHV is as given in Eq. 10 (Boie 1957).

$$\begin{aligned} \text{HHV} = & 0.3516[\text{C}] + 1.16225[\text{H}] \\ & + 0.10465[\text{S}] - 0.11090[\text{O}] - 0.0628[\text{N}] \\ & + 0.10465\text{S} \end{aligned} \quad (5)$$

$$\text{HHV} = 0.2949[\text{C}] + 0.825[\text{H}] \quad (6)$$

$$\begin{aligned} \text{HHV} = & -0.763 + 0.301[\text{C}] + 0.525[\text{H}] \\ & + 0.064[\text{O}] \end{aligned} \quad (7)$$

$$\text{HHV} = 0.196[\text{FC}] + 14.119 \quad (8)$$

$$\text{HHV} = 0.1905[\text{VM}] + 0.2521[\text{FC}] \quad (9)$$

$$\text{LHV (MJ/kg)} = \text{HHV} - \text{hg} (9\text{H}/100 + \text{M}/100) \quad (10)$$

LHV in Eq. 10 is lower heating value of raw biomass, hg is the latent heat of steam (2.26 MJ/kg), H is hydrogen present, M is the moisture present (Basu 2010).

Characterization of raw and pretreated materials

Raw sample was quantified in terms of cellulose, hemicellulose, ash and extractives contents (Ayeni et al. 2013a, b; Blasi et al. 1999; Li et al. 2004). Extractives content was determined by using 300 mL acetone on 5 g of dry biomass in a Soxhlet extractor. Extraction was carried out for 4 h run period with the heating temperature maintained at 70 °C. The extractives content was calculated as the difference in weight between raw and extracted materials at 105 °C oven temperature (Ayeni et al. 2013b; Blasi et al. 1999). Lignin (soluble and insoluble) as well as ash contents were established by the NREL methods (Sluiter et al. 2008, 2012). Lignin composition was determined by weighing into glass test tubes 0.3 g of dry extracted biomass and adding 3 mL of 72% H₂SO₄ and allowing hydrolysis to occur at 23 °C for 2 h. The second hydrolysis step was carried out in an autoclave for 1 h at 121 °C. The hemicellulose content was determined by placing 1 g of dried biomass from the extractive analysis into a 250 mL Erlenmeyer flask and then 150 mL of 500 mol/m³ NaOH solution was added. The mixture was boiled for 3 h and 30 min in a water bath. The residue was dried to a constant weight at 105 °C and later cooled in a desiccator and weighed. The difference between the sample weight before and after this treatment is the hemicellulose (Ayeni et al. 2013b; Li et al. 2004). The cellulose content was calculated by difference with the assumption that extractives, hemicellulose, lignin, ash, and cellulose are the only components of the entire biomass (Ayeni et al. 2013a, b; Blasi et al. 1999; Li et al. 2004). The pretreated samples were further characterized as cellulose retained, hemicellulose solubilized, and lignin removed in the solid pretreated fractions as established previously (Ayeni et al. 2013a, 2016a; Ayeni and Daramola 2017) (Table 1).

Stereomicroscopy imaging

Air dried samples of the untreated, pretreated, and enzyme digested, and SSF rice husks biomass were subjected to stereomicroscopy imaging. The samples were placed on a black background and images were captured using a Nikon SMZ745T stereomicroscope equipped with NIS-Element D Z-Series 7 software (Ayeni and Daramola 2017). The Nikon DS-Fi2 CCD camera was operated by a Nikon Digital Sight System.

Scanning electron microscopy (SEM) imaging

The untreated, alkaline peroxide oxidation treated, enzymatic and SSF treated biomass of rice husks samples were washed with distilled water and air dried for 72 h, and later stored in capped 50 mL-sized conical plastics for SEM analysis. The air-dried samples were mounted on aluminium stubs using conductive carbon tape followed by sputter coating with carbon and gold–palladium at 5 nanometre scale. Biomass samples were examined using FEI Quanta 200 scanning electron microscope operated under vacuum between 3.9×10^{-4} to 2.2×10^{-3} Pascals with a voltage of 30 kV.

Fourier Transform Infrared spectroscopy

Infrared frequencies correspond to vibrational modes in specific chemical bonds. The stronger the bonds, the higher the frequency the atoms vibrate. Fourier transform infrared (FTIR) spectroscopy was carried out on the raw, pretreated, enzyme digested, and fermented treated rice husk biomass using a Bruker FTIR spectrophotometer in order to determine the presence of functional groups and obtaining precise information related to the structure of cellulose molecules through parameters like the nature of hydrogen bonding index (HBI, which is due to the O–H stretching vibrations from alcohols and carboxylic acids present either in lignin and polysaccharides) or its crystallinity indices (Lateral order index, LOI (corresponding to a CH₂ bending vibrations), and total crystallinity index, TCI (corresponding to the C–H stretching). The ratios of the absorption bands at 2900, 1437, 1378, and 899 cm⁻¹ were considered for both LOI and TCI, while HBI was observed at the absorption bands ratio of 3400 and 1320 cm⁻¹. Pellet technique was used where dried biomass samples were mixed with KBr and pressed under vacuum to form pellets. The FTIR spectral analysis was performed within the wave number range of 4000–500 cm⁻¹ using 64 scans with baseline corrections (Nelson and O'Connor 1964; Spiridon et al. 2011; Bian et al. 2012).

Results and discussion

Proximate and ultimate values of raw biomass

The results obtained for the proximate and ultimate analysis are presented in Table 2 along with the caloric values of the raw biomass. The information on thermo-decomposition ability of lignocellulosic biomass can be provided through proximate and ultimate analysis. These are excellent indicators of biomass quality for bioprocessing, assessing the fuel characteristics and bio-commodity potentials. The moisture content was 4.97%, indicating the suitability of the rice husks for fuels and chemicals production. Permych and Koupryanov (2004), reported that biomass with moisture content below 50% is effectively used in combustion. High moisture promotes rapid microbial respiration activity thereby deteriorating the physical quality of the fuel and pyrolysis gases. Moisture content negatively impacts overall energy balance and

Table 2 Proximate, ultimate, and heating values of raw rice husks biomass

Proximate (wt% dry basis)		
Moisture		4.97
Volatile matter		67.27
Fixed carbon		14.13
Ash		13.63
Ultimate (wt% dry basis)		
C		38.70
H		5.80
N		0.35
O		41.39
S		0.13
Higher heating value (MJ/kg)		
Experimental	Calculated from Eqs. 5 to 9	Difference (%)
16.20	15.75	2.8
	16.20	0
	16.58	2.35
	16.89	4.26
	16.38	1.11
Lower heating value (MJ/kg) ^a		
14.90		

^a Calculated from Eq. 10

general process economics (Wright et al. 2010). The volatile matter content was 67.27%, showing high reactivity of biomass. Volatile matter is composed of short and long chain hydrocarbons, aromatic hydrocarbons which are viable precursors for fuels and some other platform chemicals. Ash (the inorganic part of the biomass left after complete combustion) content was high (about 14%) which must have contributed to the low carbon content (38.70%). Ash may cause decrease in yield and heating values and harmful deposits which may cause thermal resistance and imply extensive maintenance. The amount of volatile matter in biomass depends on the type of fuel and is inversely proportional to water and ash content of the fuel. The raw biomass can be considered having negligible sulphur (0.13%) and nitrogen (0.35%) compositions (Table 2). The low levels indicate that SO₂ and NO_x emissions are negligible during combustion or processing. High level of sulphur contents in biofuels generates SO₂ that forms sulphates, generating ashes. The percent difference of the experimental HHV (16.20 MJ/kg) and calculated HHV values varied from 0 to 4%, showing the usefulness of the chosen correlations in predicting HHV from the experimental proximate and ultimate values.

Compositional analysis of raw and pretreated solid fraction

The raw and pretreated solid samples for all the experimental runs were estimated for polysaccharides (cellulose and hemicellulose) and lignin contents. The pretreatment method applied in this study was aimed at fractionating the rice husks into solid fraction containing as much cellulose and as less lignin. Table 1 shows the compositions of the raw and treated biomass. The treated biomass was estimated based on the cellulose content, hemicellulose solubilized, and lignin removal (delignification). The compositional analysis of the raw sample shows (Table 1) a total polysaccharide content of 64% (w/w), lignin content of about 22% (w/w), and extractives and ash contents totalling 14% (w/w). These evaluations agree closely to some other published studies (Hsu et al. 2010; Banerjee et al. 2009; Dagnino et al. 2013). Lignocelluloses are recalcitrant to enzymatic saccharification due to their complex nature. The cellulose is crystalline in structure together with the amorphous nature

of the hemicellulose locked up together with the lignin sheath. Therefore, a solid fraction containing more polysaccharides and less of the lignin increases the yield of fermentable sugars during enzymatic digestibility. In this study, the cellulose content in the pretreated biomass (pretreatment 2) was enhanced to about 56% from an initial raw biomass cellulose content of 38% and to about 72% polysaccharide content from an initial raw content of about 64% (Table 1). The ash and extractives contents increased as a result of the reduction in lignin contents after pretreatments (pretreatments 6, 7, and 8). The reduction of the lignin contents was more pronounced at higher temperature (120 °C) and shorter time (1 h) (Table 1). Pretreatments at elevated temperatures and longer time result in biomass charring (McGinnis et al. 1984). This is because cellulose get degraded at much higher temperatures. In addition, at elevated temperatures, more lignin can be removed. Therefore, a shorter pretreatment time at reasonable elevated temperatures results in more lignin reduction with less cellulose degradation (McGinnis et al. 1984; Ayeni et al. 2013b). It can be noticed from Tables 1 and 3 that cellulose contents were enhanced at lower temperature of 100 °C than at increased temperature of 120 °C. It has been reported that cellulose gets degraded at elevated temperatures thereby releasing degradation products into the pretreatment hydrolysate which may hinder the production of fermentable sugars or ethanol (Dagnino et al. 2013; McGinnis et al. 1984). The degradation of cellulose

can result in economic and processing implications (Dagnino et al. 2013). Therefore, wide range of options for controlling the pretreatment conditions to meet the requirements of a desired process are to be considered. Hemicellulose solubilization varied from 46% (w/w) (pretreatment 7; 120 °C, 1 h, 1% H₂O₂) to maximum of 70% (w/w) (pretreatment 1; 100 °C, 2 h, 3% H₂O₂). With the same trend, lignin removal was highest in pretreatment 1 (68% (w/w); 100 °C, 1 h, 3% H₂O₂). The lowest value for delignification was 41% (w/w) (pretreatment 2; 100 °C, 2 h, 1% H₂O₂).

The regression equations relating the cellulose content, hemicellulose solubilisation, and lignin removal to the operating variables of temperature (A), time (B) and hydrogen peroxide concentration (C) can be written as follows:

$$\begin{aligned} \text{Cellulose content \% (w/w)} \\ = 69.0 - 0.275A + 25.00B - 9.25C - 0.1500AB \\ + 0.1000AC - 2.500BC \end{aligned} \quad (11)$$

$$R^2 = 92.97 \quad (R^2 \text{ adjusted} = 87.47)$$

$$\begin{aligned} \text{Hemicellulose solubilization \% (w/w)} \\ = 98.75 - 0.700A - 16.500B + 18.375C \\ + 0.32500AB + 0.01250AC - 11.2500BC \end{aligned} \quad (12)$$

$$R^2 = 99.97 \quad (R^2 \text{ adjusted} = 99.95)$$

Table 3 2³ Factorial design experimental matrix, experimental and predicted responses for cellulose contents, hemicellulose solubilization, and lignin removal (%w/w)

Run order	Temp. (°C)	Time (h)	H ₂ O ₂ (%v/v)	Experimental values			Predicted values		
				Cellulose content	Hemicellulose solubilization	Lignin removal	Cellulose content	Hemicellulose solubilization	Lignin removal
1	100	1	3	45	70	68	47	70	65
2	100	2	1	56	58	41	57	58	38
3	120	2	1	49	57	51	48	57	54
4	100	2	3	50	52	45	49	52	48
5	100	1	1	51	53	51	50	53	54
6	120	2	3	42	52	67	43	52	64
7	120	1	1	42	46	55	43	46	52
8	120	1	3	45	63	60	44	63	63

$$\begin{aligned} \text{Lignin removal \% (w/w)} = & 165.5 - 1.000A \\ & - 106.5B + 5.250C \\ & + 0.900AB \end{aligned} \quad (13)$$

$$R^2 = 89.11 \quad (R^2 \text{ adjusted} = 85.14)$$

Statistical analysis of results

Effect of operating variables on pretreatment yields was validated using the analysis of variance

(ANOVA) method (Table 4). High coefficients of determination (R^2) for the three responses of cellulose content, hemicellulose solubilisation, and lignin removal were 92.97, 99.95, and 89.11% respectively (Eqs. 11–13). The correlations of the predicted and experimental responses of the cellulose content, hemicellulose solubilization, and lignin removal are shown in Table 5. A higher coefficient of determination showed a higher reliability regarding the relationship between the experimental and predicted values. Variables with coefficients having a level of

Table 4 Analysis of variance (ANOVA) for the polynomial models obtained from experimental design

Source	DF ^a	Seq SS ^b	Adj SS ^c	Adj MS ^d	F-Value	p Value
<i>Cellulose content</i>						
Model	6	307.00	307.00	51.17	18.42	0.0000
Linear	3	257.00	257.00	85.67	30.84	0.0000
A	1	257.00	144.00	144.00	51.84	0.0000
B	1	49.00	49.00	49.00	17.64	0.0020
C	1	64.00	64.00	64.00	23.04	0.0010
Interactions	3	50.00	50.00	16.67	6.00	0.0160
AB	1	9.00	9.00	9.00	3.24	0.1050
AC	1	16.00	16.00	16.00	5.76	0.0400
BC	1	25.00	25.00	25.00	9.00	0.0150
Error	9	25.00	25.00	2.78		
<i>Hemicellulose Solubilization</i>						
Model	6	779.5	779.5	129.917	4677	0.0000
Linear	3	230.75	230.75	76.917	2769	0.0000
A	1	56.25	56.25	56.25	2025	0.0000
B	1	42.25	42.25	42.25	1521	0.0000
C	1	132.25	132.25	132.25	4761	0.0000
Interactions	3	548.75	548.75	182.917	6585	0.0000
AB	1	42.25	42.25	42.25	1521	0.0000
AC	1	0.25	0.25	0.25	9	0.0150
BC	1	506.25	506.25	506.25	18225	0.0000
Error	9	0.25	0.25	0.028		
<i>Lignin removal</i>						
Model	6	1187.00	1187.00	197.83	12.36	0.0010
Linear	3	862.00	862.00	287.33	17.96	0.0000
A	1	196.00	196.00	196.00	12.25	0.0070
B	1	225.00	225.00	225.00	14.06	0.0050
C	1	441.00	441.00	441.00	27.56	0.0010
Interactions	3	325.00	325.00	108.33	6.77	0.0110
AB	1	324.00	324.00	324.00	20.25	0.0010
AC	1	0.00	0.00	0.00	0.00	1.0000
BC	1	1.00	1.00	1.00	0.06	0.8080
Error	9	144.00	144.00	16.00		

^a Degree of freedom, ^b sequential sum of squares, ^c adjusted sum of squares, ^d adjusted mean square

Table 5 Correlations of predicted and experimental values of cellulose content, hemicellulose solubilization, and lignin removal

Component	Correlation ^a	R^2
Cellulose	$Y = 0.9247X + 3.7018$	0.9346
Hemicellulose solub.	$Y = X$	1.0000
Lignin removal	$Y = 0.8918X + 5.9234$	0.8918

Y = Predicted values. X = Experimental values

^a The correlations were used in order to evaluate the residuals of the experimental and the predicted values according to Eqs. 2 and 3. The residual values were within the allowable ranges

significance adjustment of 95% were considered in the three equations. R^2 values for the three responses were higher than 80% (89–100%), which ensures satisfactory fitness of the regression models with the experimental data. Furthermore, it was observed that the experimental R^2 values were in reasonable agreement with the adjusted R^2 values (Eqs 11–13). The summary of analysis of variance representing the results indicate that the three models generated from the experimental data are highly significant ($P \leq 0.001$) on the three responses and are presented in Table 4. All linear factors (temperature, time, and % H_2O_2) are highly significant on the three responses ($P \leq 0.007$). The two-way interactions (interactions of the factors) also indicated high significance on the three responses ($P \leq 0.016$). The linear as well as the two-way interactions also have high F -values. The most effective factor on cellulose content was the linear effect of temperature (F -value = 51). The two-way interactive effect of time and H_2O_2 was the highest on hemicellulose solubilisation (F -value = 18.23) while temperature and time interactive effect on lignin removal was the highest (F -value = 20.25). The hydrogen peroxide linear effect on lignin removal was highly significant ($P \leq 0.0010$). The Pareto charts further showed the significant linear and interactive effects on the responses (Fig. 1).

From Fig. 1a, temperature, time, and % H_2O_2 as well as their interactive effects influenced enhance cellulose in the treated biomass. Further, Fig. 1b shows the linear and all the interactive effects influenced hemicellulose solubilisation. The three linear effects and only temperature and time interactive effect influenced lignin removal (Fig. 1c).

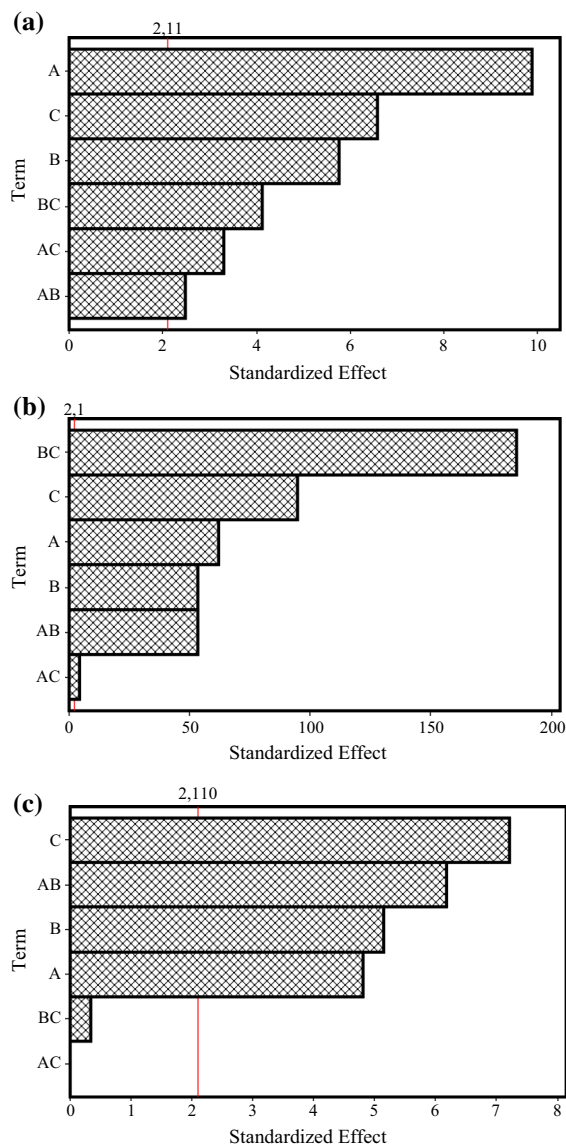


Fig. 1 Pareto chart of effects on cellulose content (a), hemicellulose solubilization (b), and lignin removal (c)

Optimization and validation of the pretreatment process

The multi-response optimization problem was solved through the desirability function (Dagnino et al. 2013). The desirability function approach simultaneously optimizes multiple equations and translates the functions to a common scale (Dagnino et al. 2013). This function was used to maximize the cellulose content, hemicellulose solubilisation, and lignin removal. Desirability of the responses varied between 0.7 and

1.0 corresponding to optimal conditions. Two-dimensional contour plot and three-dimensional response surface curves (Fig. 2) were plotted to study the interactions between the various parameters on the responses to determine the optimum levels of each factor required to obtain maximum responses.

The shape of the response plots indicated the nature and extent of the interactions between the different factors (Lee et al. 2007; Jung et al. 2011). The model equations for the responses (Eqs. 11–13) together with the contour and surface response plots were utilized in determining the optimum conditions to obtain a solid

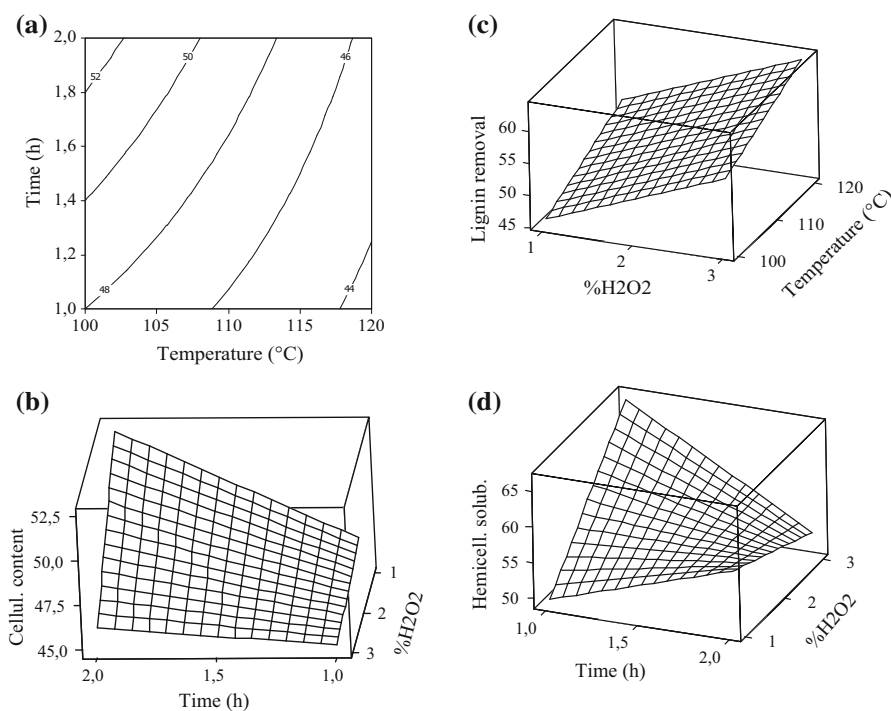
fraction with high cellulose content, low lignin and hemicellulose contents. Considering these constraints, the optimum cumulative responses (52% cellulose content, 57% hemicellulose solubilisation, and 47% lignin removal) were obtained at 109 °C, 2 h, and 1.38% H₂O₂ pretreatment conditions. To validate the experiments, additional sets of experiments at these specific conditions were performed. Results after validation produced 56% (w/w) cellulose content, 55% (w/w) hemicellulose solubilisation, and 48% (w/w) lignin removal. The experimental and predicted responses were found to be in close agreement, thus confirming the optimization process.

Enzymatic digestibility of treated biomass to fermentable sugars

Enzyme convertibility of pretreated (at the validated optimized conditions: 109 °C, 2 h, and 1.38% H₂O₂) rice husks biomass at fixed loading of 2% was studied in more detail as a function of enzyme dosages and digestion period. The economic viability of the enzymatic hydrolysis process is governed by efficient cellulase loadings (Yang and Wyman 2008). The reducing sugars yield decreased with increasing cellulase enzyme loading (Fig. 3). Sugar yields of the pretreated biomass was significantly higher than the untreated biomass (maximum at 43 mg/g biomass after the fourth day (Fig. 3).

Cellulase loading at 35 FPU/g cellulose exhibited the highest increase in reducing sugars production (264 mg/g biomass) after 72 h. This closely agreed with the report of Yang and Wyman 2008 that enzymatic hydrolysis ideally reaches the peak at the end of the third day. The enzymatic conversion process data generally showed that increasing enzyme loadings beyond 35 FPU/g cellulose is not economical for the process. The reduction in the production of reducing sugars at high cellulase loadings may have been caused by oversaturation of the cellulolytic sites

Fig. 2 Contour plot and surface plots for cellulose content, lignin removal and hemicellulose solubilization. **a** Contour plot of cellulose content (%w/w) versus time and temperature; **b** surface plot of cellulose content (%w/w) versus time and % H₂O₂; **c** surface plot of lignin removal (%w/w) versus temperature and % H₂O₂; **d** surface plot of hemicellulose solubilization (%w/w) versus Time and % H₂O₂



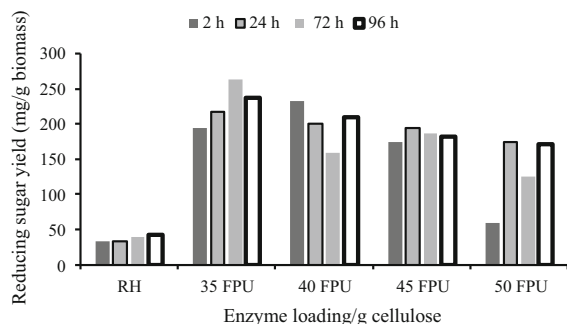


Fig. 3 Reducing sugar yield with variation in cellulase enzymes loadings at constant biomass loading of 2%. RH = Raw rice husks, was hydrolysed at 35 FPU/g cellulose loading

by the cellulase enzyme complex. By inference, there were more competitions of the enzymes with available substrates in the medium. In addition, end products of enzymatic hydrolysis such as cellobiose, glucose, and some forms of furan compounds may also inhibit enzyme activities which negatively affects cellulose hydrolysis (Andric et al. 2010). A critical feature of an effective pretreatment is high sugar yields at low enzyme loadings.

In order to study the effect of substrate inhibition on biomass conversion to sugars, the reducing sugars yields with variation in biomass loadings revealed some interesting information on the digested treated biomass. It should also be noted that the degree of substrate inhibition is largely affected by the ratio of quality of substrate to that of the enzyme. In Fig. 4, at increasing biomass loadings (e.g. 2, 3, and 5%), reducing sugars production increased progressively up to the end of 24 h and reduced as the hydrolysis

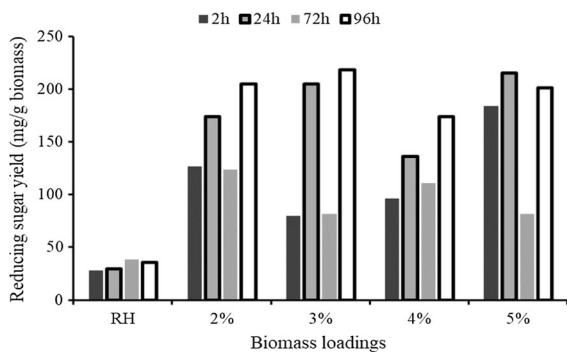


Fig. 4 Reducing sugar yields with variation in biomass loadings and enzyme loading of 35 FPU/g cellulose. RH = Raw rice husks loading was fixed at 2% biomass loading

periods increased. For example, at 3% loading after the first day, sugar yield was 205 mg/g dry biomass, while at 5% loading after the first day, sugar yield was 216 mg/g dry biomass. Considering biomass loading at 3% and hydrolysis period of 96 h, reducing sugars production was highest (218 mg/g dry biomass) (Fig. 4). With the foregoing, we can conclude that increased reducing sugars was produced at increased biomass loading but at very short hydrolysis period (24 h). On the other hand, more of the reducing sugars was produced at lower biomass loadings (2 and 3%) but at longer periods. Increasing biomass loading for longer period could lead to end product inhibition, other inhibitors, or inefficient mixing (Ayeni et al. 2016a). Therefore, considering the process economics, shorter hydrolysis period and lower biomass loading should be the preferred option, i.e., 3% biomass loading at the end of the first day (sugar yield of 205 mg/g) and at cellulase loading of 35 FPU/g cellulose. Tengborg et al. 2001 reported that sources of raw material and enzyme are connected to the temperature, pH, as well as the hydrolysis residence time.

The pretreated biomass at the validated optimized conditions (Temperature: 109 °C; Time: 2 h; % H₂O₂: 1.38, validating 56% cellulose content, 55% hemicellulose solubilization, and 48% lignin removal) was used to evaluate the SSF process. The ethanol produced from the substrates was increased rapidly in the initial stage, while the conversion rate progressively reduced as the reaction proceeded (Figs. 5, 6). Results showed that ethanol production increased progressively for the 96 h period (Fig. 5). In addition, glucose production increased up to 149 g/L (giving rise to the highest ethanol production of 24 g/

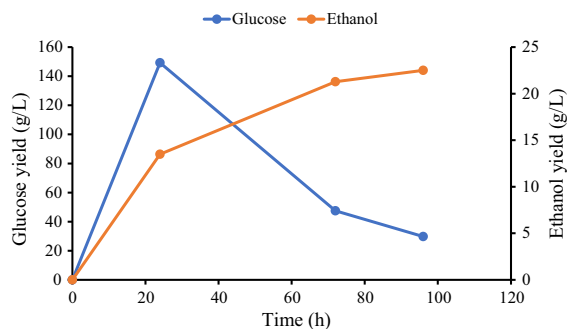


Fig. 5 Ethanol production and glucose depletion during SSF process

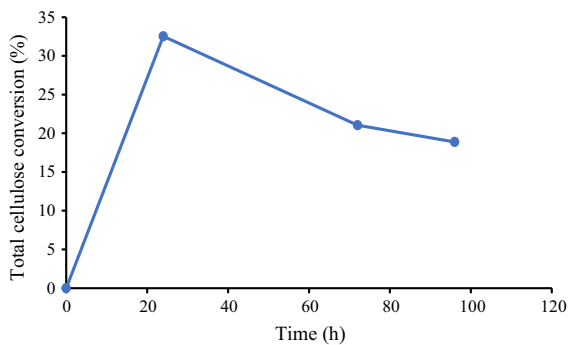


Fig. 6 Total cellulose conversion rate of pretreated sample at optimized conditions after SSF at 3% solid loading, 35 FPU/g cellulose loading for 96 h

L) at the end of the first day and there was a gradual depletion to the fourth day. This may be due to the reduction of available sugar as a result of the increasing microbial population thereby giving rise to substrate or microbial inhibition. Product inhibition (caused by accumulated sugar) may also be a factor in the reduction of cellulose reduction rate. The glucose depletion may also have been caused by lack of available water (Xing et al. 2016). Strong water absorption action may occur during the SSF process resulting in lack of free water thereby reducing mixing and handling of the fermenting medium (Xing et al. 2016). Figure 6 confirms the reduction in the total cellulose conversion rate as the available sugars in the medium became depleted with time. The highest cellulose conversion (33%) occurred at the end of the first day (confirming that the best reducing sugars production conditions should be at lower biomass loading and shorter hydrolysis period) and reduced to about 19% at the end of the fourth day.

Physical features of raw and treated biomass

The stereomicroscopy images (Fig. 7) show the loosed particles (raw samples; Fig. 7a), the clumped particles after pretreatment (Fig. 7b), enzymatic hydrolysis (Fig. 7c), and SSF stages (Fig. 7d). The images show gradual changes in colour and particle size arrangements from the raw samples to the downstream processing of SSF biomass. From the dark brown colour and well loosed sizes of the raw samples to the light brown colour of the pretreated samples (caused by the bleaching action of H_2O_2) to the more compact, darker colourations of the enzyme

hydrolysed and SSF samples (caused by the digestions of the samples by cellulases and microbes during fermentation step). The stereomicrography images also show a general trend of particle size reduction with increasing number of smaller and thin fibers for the pretreated, enzymatic hydrolysed, SSF samples. Clumping or variability of treated particles after pretreatment could be attributed to the changes in surface morphology, area, and energy. This may have been brought about by the relocalization of lignin to the particle surface (Ayeni and Daramola 2017; Donohoe et al. 2008; Chundawat et al. 2011). Smaller particles increase surface area thereby leading to increased enzymatic digestibility (Ayeni and Daramola 2017; Ciesielski et al. 2014; Stasolla et al. 2003). Mixing is also increased with smaller particles than larger particles (which reduces the consistency during pretreatment and SSF) (Ayeni and Daramola 2017; Ciesielski et al. 2014; Stasolla et al. 2003; Viamajala et al. 2009).

Structural and morphological evaluation of raw and treated biomass

The scanning electron microscopy was employed for morphological inspection. Figure 8 show the SEM micrographics of the raw, pretreated (at the optimized conditions), enzyme hydrolysed, and SSF rice husks biomass. The structural and morphological evaluations as well as the FTIR measurements for the enzyme hydrolysed and SSF were inspected on the samples studied at 3% dry biomass loading and 35 FPU/g cellulose loading. Bian et al. (2012) proposed that changes of morphology brought about by downstream processing on the raw biomass are due to the removal of hemicelluloses and a small amount of amorphous cellulose. From the compositional analysis results of the treated biomass (Table 3), hemicellulose solubilization was as high as 70% (Pretreatment 1) showing the relationship between surface deformations and hemicelluloses removal (Fig. 8a–d). Figure 8b, c clearly show a well disrupted microfibrils. Looking at the surface closely for the SSF process, it can be noted that the well-ordered structures of the raw biomass (Fig. 8a) have been completely eroded and disrupted. Furthermore, in the lignocellulosic complex, hemicelluloses play the role of regulator influencing the aggregation of cellulose into fibril and fibril aggregates during biogenesis of cell wall in plants

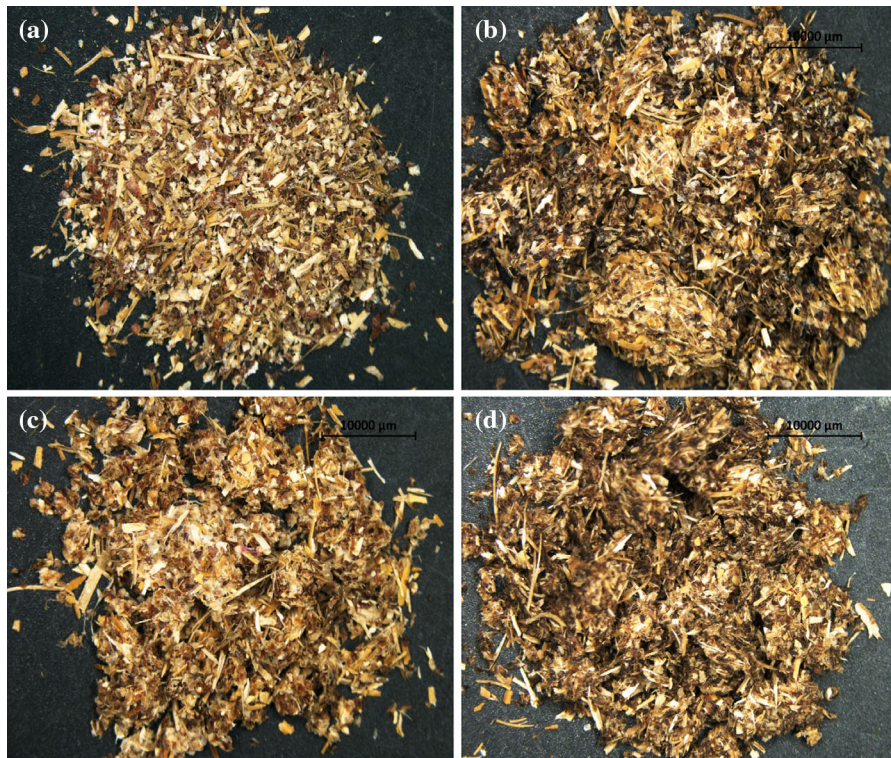


Fig. 7 Stereoscope micrographs taken at 10,000 μm scale of the untreated (a), Pretreated (b), Enzyme hydrolyzed treated biomass (c) and SSF hydrolysed pretreated (d) rice husks

biomass. Readers are referred to the online version of this article for proper interpretation of the images

(Tokoh et al. 1998). Therefore, during treatments, the hemicellulose integrated into the cellulose structure and within and between the cellulose fibrils are removed which disrupt the intact and smooth surface of the microfibrils thereby leading to bends, deeps, and twists (Bian et al. 2012).

FTIR measurements

Fourier transform infra-red (FTIR) spectroscopy determines crystallinity index (CI) by measuring relative peak heights or areas (Akerholm et al. 2004) using the mechanism of spectrum contributions from the crystalline and amorphous regions. FTIR is the simplest method for measuring crystallinity index (Park et al. 2010). In this study, the ratios LOI, TCI, and HBI (Spiridon et al. 2011; Nelson and O'Connor 1964) were used to accessed the degree of crystallinity (Table 6). Table 6 shows a gradual but not pronounced increase of LOI ratio of the treated (1.08) to the SSF (1.22). Many factors affect the enzyme

digestibility of treated and untreated lignocellulosic biomass. The degradation of crystalline cellulose generally involves the action of both endo- and exo-acting cellulases (Wang et al. 2013; Ayeni et al. 2016b). During pretreatment, enzymatic hydrolysis, and SSF periods, the higher crystallinity and ordered structure of the native biomass is transformed into mostly amorphous forms. The lignocellulosic complex is thereby fragmented and the porosity is further increased. The increased amorphous surfaces provide for more enzyme or microbial attack. The LOI values tended to increase for the enzyme and SSF treated samples compared to the raw biomass (Table 6). The ordered crystalline structures and regular degree of intermolecularity of substrates were affected by the collapse of the fibre structures. Furthermore, comparing the raw, pretreated, enzyme hydrolysed, and SSF samples at the same wavenumbers to the %Transmittance, there were pronounced reductions in transmittance from as high as 91% HBI for raw sample to as low as 76% HBI for enzyme hydrolysed samples, and

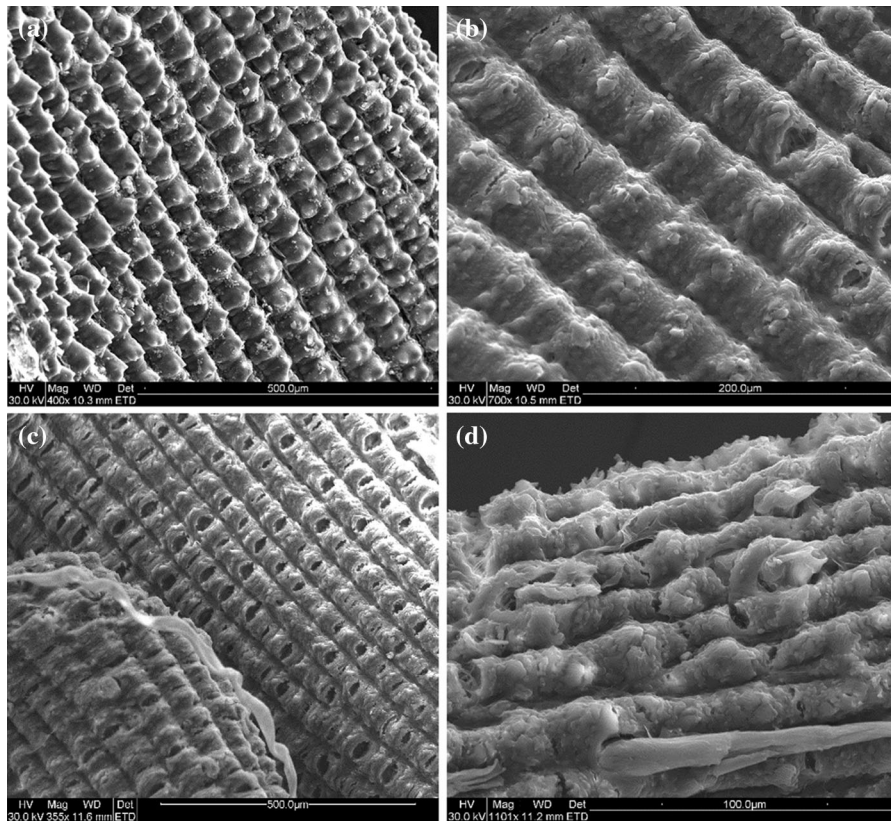


Fig. 8 SEM images of **a** raw biomass, **b** pretreated biomass, **c** Enzyme hydrolysed pretreated biomass and **d** SSF hydrolysed samples

Table 6 Infrared crystallinity ratio and hydrogen bond intensity of raw, treated, enzyme hydrolysed, and SSF of rice husks biomass

Biomass	Infrared crystallinity ratio		
	$\alpha_{1437 \text{ cm}^{-1}} / \alpha_{899 \text{ cm}^{-1}}$ (LOI)	$\alpha_{1378 \text{ cm}^{-1}} / \alpha_{2900 \text{ cm}^{-1}}$ (TCI)	$\alpha_{3400 \text{ cm}^{-1}} / \alpha_{1320 \text{ cm}^{-1}}$ (HBI)
Raw	1.0833	0.9666	1.0384
Pretreated	1.0717	0.9888	1.0211
Enzyme hydrolysed	1.1111	0.8683	1.0414
SSF	1.2214	0.9246	0.8822

72% HBI for SSF samples (Figures are not shown). Similar progressions were observed for LOI and TCI values. %Transmittance shows changes corresponding to the sample composition, related to the bonds or phase or crystallinity. Therefore, we can say that during the enzyme hydrolysed and SSF processes, the crystallinity of the raw sample was affected in such a way that there were significant stretches in the bonds which was revealed by the increase or decrease in the %Transmittance.

Conclusions

This study showed the effectiveness of alkaline peroxide oxidation pretreatment methodology on rice husks biomass in order to fractionate the raw solid biomass and thereby increasing lignin removal, hemicellulose solubilization and cellulose enhancement amenable to fermentable sugars production and subsequent conversion of sugars to fuel ethanol. The model equations for the responses were used in arriving at optimum conditions of pretreatments. The

optimum cumulative responses were predicted and validated and resulted in 56% (w/w) cellulose content, 55% (w/w) hemicellulose solubilisation, and 48% (w/w) lignin removal at optimum pretreatment conditions of 109 °C, 2 h, and 1.38% H₂O₂. At the optimum pretreatment conditions, variations in biomass and enzyme loadings at different operating conditions (35 FPU/g cellulose, 3% biomass loading, hydrolysis temperature of 45 °C, and hydrolysis time of 24 h) established maximum reducing sugars production of 205 mg/g dry biomass. The highest cellulose conversion of 33% occurred at the end of the first day producing 24 g/L ethanol yield and a maximum glucose production (149 g/L). The reliable data from estimating the three chemical properties of proximate, ultimate, and high heating values informed the possible fuel quality of the rice husk biomass material. Stereomicroscopy and SEM imaging showed the effectiveness of chosen pretreatment method on the raw rice husk biomass. FTIR further revealed the reduction in the crystallinity of raw biomass after treatments.

References

- Agnemo R, Gellerstedt G (1979) Reactions of lignin with alkaline hydrogen peroxide. Part II. Factors influencing the decomposition of phenolic structures. *Acta Chem Scand B* 33:337–342
- Akerholm M, Hinterstoisser B, Salmen L (2004) Characterization of the crystalline structure of cellulose using static and dynamic FT-IR spectroscopy. *Carbohydr Res* 339:569–578
- Andrić P, Meyer AS, Jensen PA, Dam-Johansen K (2010) Reactor design for minimizing product inhibition during enzymatic lignocellulosic hydrolysis II. Quantification of inhibition and suitability of membrane reactors. *Biotechnol Adv* 28:407–425
- Asadieraghi M, Ashri WM, Daud W (2014) Characterization of lignocellulosic biomass thermal degradation and physico-chemical structure: effect of demineralization by diverse acid solutions. *Energy Convers Manag* 82:71–82
- ASTM D2015. Standard test method for gross calorific value of coal and coke by adiabatic bomb calorimeter. <https://www.astm.org/Standards/D2015.htm>
- Awosusi AA, Ayeni A, Adeleke R, Daramola MO (2017a) Effect of water of crystallization on the dissolution efficiency of molten zinc chloride hydrate salts during the pretreatment of corncob biomass. *J Chem Tech Biotechnol* 92:2468–2476
- Awosusi AA, Ayeni A, Adeleke R, Daramola MO (2017b) Biocompositional and thermodecompositional analysis of South African agro-waste corncob and husk towards production of biocommodities. *Asia Pac J Chem Eng* 12:960–968
- Ayeni AO, Daramola MO (2017) Lignocellulosic biomass waste beneficiation: evaluation of oxidative and non-oxidative pretreatment methodologies of South African corn cob. *J Environ Chem Eng* 5:1771–1779
- Ayeni AO, Banerjee S, Omoleye JA, Hymore FK, Giri BS, Deshmukh SC, Pandey RA, Mudliar SN (2013a) Optimization of pretreatment conditions using full factorial design and enzymatic convertibility of shea tree sawdust. *Biomass Bioenergy* 48:130–138
- Ayeni AO, Hymore FK, Mudliar SN, Deskmukh SC, Satpute DB, Omoleye JA, Pandey RA (2013b) Hydrogen peroxide and lime based oxidative pretreatment of wood waste to enhance enzymatic hydrolysis for a biorefinery: process parameters optimization using response surface methodology. *Fuel* 106:187–194
- Ayeni AO, Omoleye JA, Mudliar SN, Hymore FK, Pandey RA (2014) Utilization of lignocellulosic waste for ethanol production: enzymatic digestibility and fermentation of pretreated shea tree sawdust. *Korean J Chem Eng* 31:1180–1186
- Ayeni AO, Omoleye JA, Hymore FK, Pandey RA (2016a) Effective alkaline peroxide oxidation pretreatment of shea tree sawdust for the production of biofuels: kinetics of delignification and enzymatic conversion to sugar and subsequent production of ethanol by fermentation using *Saccharomyces cerevisiae*. *Braz J Chem Eng* 33:33–45
- Ayeni AO, Ogu R, Awosusi AA, Daramola MO (2016b) Alkaline peroxide oxidation pretreatment of corn cob and rice husks for bioconversion into bio-commodities: Part A-Enzymatic convertibility of pretreated rice husks to reducing sugar. In: 24th European biomass conference and exhibition, pp 1225–1232. Amsterdam, Netherlands
- Bailey CW, Dence CW (1969) Reactions of alkaline hydrogen peroxide with softwood lignin model compounds. *Tappi J* 52:491–500
- Banerjee S, Sen R, Pandey R, Chakrabarti T, Satpute D, Giri B, Mudliar SN (2009) Evaluation of wet air oxidation as a pretreatment strategy for bioethanol production from rice husk and process optimization. *Biomass Bioenergy* 33:1680–1686
- Bartos C, Kukovec Á, Ambrus R, Farkas G, Radacs N, Szabó-Révész P (2015) Comparison of static and dynamic sonication as process intensification for particle size reduction using a factorial design. *Chem Eng Process* 87:26–34
- Basu P (2010) Biomass gasification and pyrolysis: practical design and theory. Elsevier, Oxford
- Bennet C (1971) Spectrophotometric acid dichromate method for the determination of ethyl alcohol. *Am J Med Technol* 37:217–220
- Bian J, Peng F, Peng X-P, Peng P, Xu F, Sun R-C (2012) Acetic acid enhanced purification of crude cellulose from sugarcane bagasse: structural and morphological characterization. *Bioresources* 7:4626–4639
- Binder JB, Raines RT (2010) Fermentable sugars by chemical hydrolysis of biomass. *Proc Natl Acad Sci USA* 107:4516–4521
- Blasi CD, Signorelli G, Russo CD, Rea G (1999) Product distribution from pyrolysis of wood and agricultural residues. *Ind Eng Chem Res* 38:2216–2224

- Boie W (1957) Vom Brennstoff zum Rauchgas, in: Feuerungstechnisches Rechnen mit Brennstoffkenngrößen und seine Vereinfachung mit Mitteln der Statistik, Teubner, Leipzig
- Buzala K, Przybysz P, Rosicka-Kaczmarek J, Kalinowska H (2015) Production of glucose-rich enzymatic hydrolysates from cellulosic pulps. *Cellulose* 22:663–674
- Chang VS, Nagwani M, Holtzapfel MT (1998) Lime pretreatment of crop residues bagasse and wheat straw. *Appl Biochem Biotechnol* 74:135–159
- Chundawat SPS, Donohoe BS, Sousa LD, Elder T, Agarwal UP, Lu F, Ralph J, Himmel ME, Balan V, Dale BE (2011) Multi-scale visualization and characterization of lignocellulosic plant cell wall deconstruction during thermochemical pretreatment. *Energy Environ Sci* 4:973–984
- Ciesielski PN, Wang W, Chen X, Vinzant TB, Tucker MP, Decker SR, Himmel ME, Johnson DK, Donohoe BS (2014) Effect of mechanical disruption on the effectiveness of three reactors used for dilute acid pretreatment of corn stover Part 2: morphological and structural substrate analysis. *Biotechnol Biofuels* 7:47
- Dagnino EP, Chamorro ER, Romano SD, Felissia FE, Area MC (2013) Optimization of the acid pretreatment of rice hulls to obtain fermentable sugars for bioethanol production. *Ind Crops Prod* 42:363–368
- Demirbas A (1997) Calculation of high heating values of biomass fuels. *Fuel* 76:431–434
- Donohoe BS, Decker SR, Tucker MP, Himmel ME, Vinzant TB (2008) Visualizing lignin coalescence and migration through maize cell walls following thermochemical pretreatment. *Biotechnol Bioeng* 101:913–925
- Dowe N, McMillan J (2008) SSF experimental protocols: Lignocellulosic biomass hydrolysis and fermentation LAP. NREL/TP-510-42630. Contract No.: DE-AC36-99-GO10337
- El-Sayed SA, Mostafa ME (2015) Kinetic parameters determination of biomass pyrolysis fuels using TGA and DTA techniques. *Waste Biomass Valor* 6:401–415
- Fannie PE, Okafor J, Roberson C (1998) Determination of insoluble solids of pretreated biomass material. LAP-18. Version 09-23-1998
- Forney LJ, Reddy CA, Tien M, Aust SD (1982) The involvement of hydroxyl radical derived from hydrogen peroxide in lignin degradation by the white rot fungus *Phanerochaete chrysosporium*. *J Biol Chem* 257:11455–11462
- García R, Pizarro C, Lavín AG, Bueno JL (2014) Spanish biofuels heating value estimation. Part 1: Ultimate analysis data. *Fuel* 117:1130–1138
- Gould JM (1985) Studies on the mechanism of alkaline peroxide delignification of agricultural residues. *Biotechnol Bioeng* 27:225–231
- Hsu T, Guo G, Chen W, Hwang W (2010) Effect of dilute acid pretreatment of rice straw on structural properties and enzymatic hydrolysis. *Bioresour Technol* 101:4907–4913
- Jenkins BM, Ebeling JM (1985) Correlations of physical and chemical properties of terrestrial biomass with conversion. In: Proceedings of 1985 symposium energy from biomass and waste IX IGT, p 271, California
- Jeya M, Zhang Y, Kim I, Lee J (2009) Enhanced saccharification of alkali-treated rice straw by cellulase from *Trametes hirsuta* and statistical optimization of hydrolysis conditions by RSM. *Bioresour Technol* 100:5155–5161
- Jung KW, Kim DH, Kim HW, Shin HS (2011) Optimization of combined (acid + thermal) pretreatment for fermentative hydrogen production from *Laminaria japonica* using response surface methodology (RSM). *Int J Hydrog Energy* 36:9626–9631
- Kaiser S, Verza SG, Moraes RC, Pittol V, Peñaloza EMC, Pavei C, Ortega GG (2013) Extraction optimization of polyphenols, oxindole alkaloids and quinovic acid glycosides from cat's claw bark by Box-Behnken design. *Ind Crops Prod* 48:153–161
- Kim S, Dale BE (2004) Global potential bioethanol production from wasted crops and crop residues. *Biomass Bioenergy* 26:361–375
- Kutsuki H, Gold MH (1982) Generation of hydroxyl radical and its involvement in lignin degradation by *Phanerochaete chrysosporium*. *Biochem Biophys Res Commun* 109:320–327
- Lachenal D, de Choudens C, Monzie P (1980) Hydrogen peroxide as a delignifying agent. *Tappi J* 63:119–122
- Lee JH, Lim SL, Song YS, Kang SW, Park C, Kim SW (2007) Optimization of culture medium for lactosucrose (4G-β-D-Galactosylsucrose) production by *Sterigmatomyces elviae* mutant using statistical analysis. *J Microbiol Biotechnol* 17:1996–2004
- Li S, Xu S, Liu S, Yang C, Lu Q (2004) Fast pyrolysis of biomass in free-fall reactor for hydrogen-rich gas. *Fuel Process Technol* 85:1201–1211
- Mani T, Murugan P, Abedi J, Mahinpey N (2010) Pyrolysis of wheat straw in a thermogravimetric analyser: effect of particle size and heating rate on devolatilization and estimation of global kinetics. *Chem Eng Res Des* 88:952–958
- McGinnis GD, Prince SE, Biermann CJ, Lowrimore JF (1984) Wet oxidation of model carbohydrate compounds. *Carbohydr Res* 128:51–60
- Miller GL (1959) Use of dinitrosalicylic acid reagent for determination of reducing sugar. *Anal Chem* 31:426–428
- Nelson ML, O'Connor RT (1964) Relation of certain infrared bands to cellulose crystallinity and crystal lattice type. Part II. A new infrared ratio for estimation of crystallinity in cellulose I and II. *J Appl Polym Sci* 8:1325–1341
- Nikzad M, Movagharejad K, Najafpour GD, Talebnia F (2013) Comparative studies of effect of pretreatment of rice husk for enzymatic digestibility and bioethanol production. *Int J Eng* 26:455–464
- O'Sullivan AC (1997) Cellulose: the structure slowly unravels. *Cellulose* 4:173–207
- Onoji SE, Iyuke SE, Igbafe AI, Daramola MO (2017) *Hevea brasiliensis* (rubber seed) oil: modelling and optimization of extraction process parameters using response surface methodology and artificial neural network techniques. *Biofuels*. <https://doi.org/10.1080/17597269.2017.1338122>
- Park S, Baker JO, Himmel ME, Parilla PA, Johnson DK (2010) Cellulose crystallinity index: measurement techniques and their impact on interpreting cellulase performance. *Biotechnol Biofuels* 3:10
- Permchart W, Kouprianov VI (2004) Emission performance and combustion efficiency of a conical fluidized-bed combustor firing various biomass fuels. *Bioresour Technol* 92:83–91. <https://doi.org/10.1016/j.biortech.2003.07.005>

- Saha BC, Cotta MA (2007) Enzymatic saccharification and fermentation of alkaline peroxide pretreated rice hulls to ethanol. *Enzyme Microb Technol* 41:528–532
- Sarita CR, Filho RM, Costa AC (2009) Lime pretreatment of sugarcane bagasse for bioethanol production. *Appl Biochem Biotechnol* 153:139–150
- Sluiter A, Hames B, Ruiz R, Scarlata C, Sluiter J, Templeton D (2008) Determination of Ash in Biomass. LAP. NREL/TP 510-42622
- Sluiter A, Hames B, Ruiz R, Scarlata C, Sluiter J, Templeton D, Crocker D (2012) Determination of structural carbohydrates and lignin in biomass. LAP. NREL/TP 510-42618. Version 08-03-2012
- Spiridon I, Teacă C, Bodîrlău R (2011) Structural changes evidenced by FTIR spectroscopy in cellulosic materials after pretreatment with ionic liquid and enzymatic hydrolysis. *Bioresources* 6:400–413
- Stasolla C, Scott J, Egertsdotter U, Kadla J, O'Malley D, Sederoff R, Zyl L (2003) Analysis of lignin produced by cinnamyl alcohol dehydrogenase-deficient *Pinus taeda* cultured cells. *Plant Physiol Biochem* 41:439–445
- Tengborg C, Galbe M, Zacchi G (2001) Influence of enzyme loading and physical parameters on the enzymatic hydrolysis of steam pretreated softwood. *Biotechnol Progress* 17:110–117
- Tokoh C, Takabe K, Fujita M, Saiki H (1998) Cellulose synthesized by *Azotobacter xylinum* in the presence of acetyl glucosaminan. *Cellulose* 5:249–261
- Varanasi P, Singh P, Auer M, Adams PD, Simmons BA, Singh S (2013) Survey of renewable chemicals produced from lignocellulosic biomass during ionic liquid pretreatment. *Biotechnol Biofuels* 6:14
- Viamajala S, McMillan JD, Schell DJ, Elander RT (2009) Rheology of corn stover slurries at high solids concentrations—Effects of saccharification and particle size. *Bioreour Technol* 100:925–934
- Wang K, Yang H, Wang W, Sun R (2013) Structural evaluation and bioethanol production by simultaneous saccharification and fermentation with biodegraded triploid poplar. *Biotechnol Biofuels* 6:42
- Wright MM, Daugaard DE, Satrio JA, Brown RC (2010) Techno-economic analysis of biomass fast pyrolysis to transportation fuels. *Fuel* 89:S2–S10
- Xing Y, Bu L, Sun D, Liu Z, Liu S, Jiang J (2016) Enhancement of high-solid enzymatic hydrolysis and fermentation of furfural residues by addition of *Gleditsia* saponin. *Fuel* 177:142–147
- Yang B, Wyman CE (2008) Pretreatment: the key to unlocking low-cost cellulosic ethanol. *Biofuels Bioprod Biorefin* 2:26–40
- Yin C (2011) Prediction of higher heating values of biomass from proximate and ultimate analyses. *Fuel* 90:1128–1132
- Zhang Q, Cai W (2008) Enzymatic hydrolysis of alkali-pretreated rice straw by *Trichoderma reesei* ZM4-F3. *Biomass Bioenergy* 32:1130–1135